Liquid Crystals
Publication details, including instructions for authors and subscription information:
http://www.informaworld.com/smpp/title~content=t713926090

Ordered micellar and inverse micellar lyotropic phases

G. C. Shearman[a]; A. I. I. Tyler[a]; N. J. Brooks[a]; R. H. Templer[a]; O. Ces[a]; R. V. Law[a]; J. M. Seddon[a]
[a] Department of Chemistry and Chemical Biology Centre, Imperial College London, London, UK

Online publication date: 06 July 2010

To cite this Article Shearman, G. C. , Tyler, A. I. I. , Brooks, N. J. , Templer, R. H. , Ces, O. , Law, R. V. and Seddon, J. M.(2010) 'Ordered micellar and inverse micellar lyotropic phases', Liquid Crystals, 37: 6, 679 — 694
To link to this Article: DOI: 10.1080/02678292.2010.484917
URL: http://dx.doi.org/10.1080/02678292.2010.484917

Liquid Crystals,
Vol. 37, Nos. 6–7, June–July 2010, 679–694

Taylor & Francis
Taylor & Francis Group

INVITED ARTICLE

Ordered micellar and inverse micellar lyotropic phases

G.C. Shearman, A.I.I. Tyler, N.J. Brooks, R.H. Templer, O. Ces, R.V. Law and J.M. Seddon*

Department of Chemistry and Chemical Biology Centre, Imperial College London, London, UK

(*Received 4 December 2009; accepted 25 March 2010*)

In this article we review the ordered micellar and inverse micellar lyotropic liquid-crystalline phases that can be formed by amphiphilic molecules such as lipids and surfactants. We focus first on the self-assembly of amphiphiles into aggregates, and then consider the interfacial curvature and the role of curvature elasticity and packing constraints in determining the allowed structures. We then review the range of ordered micellar and inverse micellar phases that have so far been observed in a variety of surfactant and lipid systems. Finally, we describe certain characteristic properties, such as the epitaxy between phases, and the self-diffusion and electrical conductivity within such ordered micellar phases.

Keywords: amphiphiles; interfacial curvature; soft matter self-assembly; lyotropic liquid crystals; cubic phases; ordered micellar phases

1. Lyotropic phase behaviour

1.1 Amphiphiles, aggregation and interfacial curvature

In this review we focus on *three-dimensionally ordered micellar* liquid-crystalline phases of amphiphilic molecules – surfactants, lipids and amphiphilic block copolymers – in aqueous solution. We will not discuss bicontinuous, sponge or mesh phases, nor micellar solutions, lyotropic nematics or the more highly ordered lyotropic lamellar phases. We will also not discuss the analogous three-dimensional (3D) ordered structures which may form in thermotropic liquid crystals in the presence of suitable organic solvents, pure block copolymer melts or in dendrimers.

Amphiphiles such as surfactants are a very large class of organic molecules having a single polar headgroup linked either directly, or via groups such as glycerol, to one or more hydrocarbon chains (bola-amphiphiles, with a polar headgroup at each end of a hydrocarbon chain region, are also known but rather rare). As shown in Figure 1, the polar headgroup can be cationic, anionic, zwitterionic or non-ionic. It can also be oligomeric, for example in the case of the polyoxyethylene surfactants, or complex glycolipids such as the gangliosides found in cell membranes. Although the term 'surfactant' tends to be reserved for simple detergents such as the alkali carboxylate soaps or the alkyl glucosides, in reality all amphiphiles are surfactants in the sense that they will adsorb strongly at interfaces, lowering the surface/interfacial tension.

Many lipids, such as phospholipids and most glycolipids, are strongly amphiphilic, although some important classes of lipids, such as cholesterol, diacylglycerols, alkanols and protonated fatty acids (see Figure 2), are too weakly polar to form any lyotropic liquid crystal phases on their own in water. However, they are able to dissolve into lyotropic liquid crystal phases of more strongly amphiphilic lipids, strongly perturbing the structure and phase stability (this will be further described in Section 1.4).

Glycero-phospholipids are chiral at carbon C2 of the glycerol group (see Figure 1). The two optical isomers should have identical physical properties and phase behaviour, although a racemic mixture need not. Glycero-glycolipids, on the other hand, are diastereomeric, and different diastereomers might in principle have different phase behaviours. However, unlike in thermotropic liquid crystals, where molecular chirality frequently leads to the formation of chiral phases, in lyotropic systems the molecular chirality tends not to manifest itself, and almost invariably lyotropic phases are non-chiral (centrosymmetric).

Above certain concentrations in water, amphiphiles will self-assemble into aggregates (micelles) so as to shield their hydrocarbon chains from contact with the water. Above this *critical micelle concentration* (cmc), the shape of the aggregate will depend upon the balance of packing forces between the headgroups and the chains. For a large, strongly polar headgroup attached to a single, relatively short hydrocarbon chain, spherical micelles will tend to be formed, at least just above the cmc. A way of visualising this

*Corresponding author. Email: j.seddon@imperial.ac.uk

ISSN 0267-8292 print/ISSN 1366-5855 online

DOI: 10.1080/02678292.2010.484917
http://www.informaworld.com

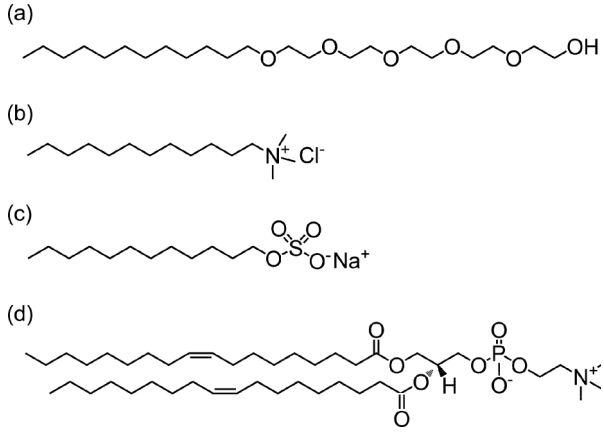

Figure 1. Examples of amphiphilic molecules: (a) non-ionic ($C_{12}EO_5$: pentaoxyethylene-*n*-dodecyl ether); (b) cationic (C_{12}TACl: dodecyl trimethylammonium chloride); (c) anionic (SDS: sodium dodecyl sulphate); (d) zwitterionic (DOPC: 1,2-*sn*-dioleoyl phosphatidylcholine).

behaviour [1, 2] is to use simple geometric considerations to assign a *packing parameter P* to the amphiphile (see Figure 3), based upon its geometric shape:

$$P = \frac{v}{a_o l_c}.$$

Here v is the molecular volume of the fluid hydrocarbon chain(s); l_c is the length of a fully extended hydrocarbon chain; and a_o is the interfacial area per molecule at the polar/non-polar interface (loosely defined as the cross-section where the polar headgroup is attached to the chains).

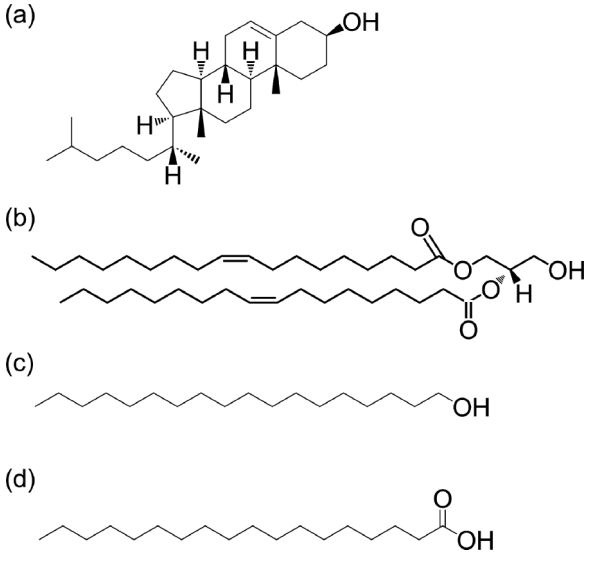

Figure 2. Amphiphilic lipids which are too weakly polar to form any lyotropic phases on their own in water: (a) cholesterol; (b) diacylglycerols (dioleoyl glycerol); (c) alkanols (octadecanol); (d) protonated fatty acids (stearic acid).

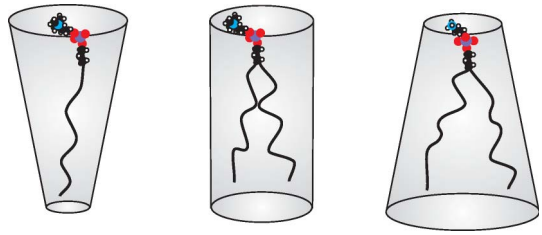

Figure 3. A cartoon showing molecules with $P < 1$, $P = 1$, $P > 1$, taken, with permission, from Shearman *et al.* [3].

From an entropic point of view, the smallest aggregate which is compatible with the packing parameter should be the favoured one, since this maximises the number of aggregates per unit volume, and hence maximises the entropy of mixing. Geometric considerations then predict the following aggregate structures with increasing packing parameter:

$P < 1/3$: spherical micelles;
$1/3 < P < 1/2$: cylindrical micelles;
$1/2 < P < 1$: flat bilayers;
$P > 1$: inverse micelles.

However, this approach is of limited quantitative value, in part because the packing parameter, P, is not a fixed quantity for a particular amphiphile, but will tend to vary strongly with parameters such as water content, temperature and pressure. Another way of trying to visualise the factors controlling the stability of lyotropic phases is to consider the balance of forces [1] within a fluid lipid bilayer.

Figure 4 emphasises that there are a range of lateral interactions acting at different depths across the bilayer. These range from repulsive steric/hydrational/electrostatic interactions between the headgroups, interfacial tension from residual water–oil contacts in any gaps between the headgroups and repulsions between the chains due to their conformational disorder.

In order for the fluid bilayer to be at mechanical equilibrium, the lateral interactions, or stress profile $t(z)$, summed across the bilayer, must add up to zero:

$$\int t(z)dz = 0. \qquad (1)$$

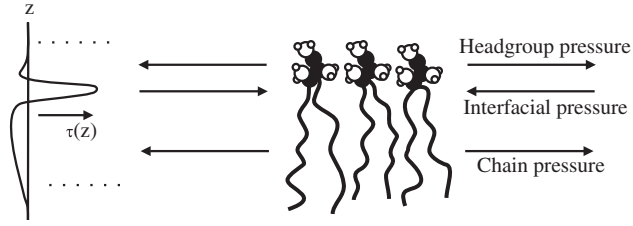

Figure 4. Balance of forces in one monolayer of a lipid bilayer, taken, with permission, from Shearman *et al.* [3].

However, it must be recognised that the two monolayers in a bilayer may prefer, energetically, to be individually curved, either away from the water or towards it. Forcing the monolayers to form a flat bilayer (under the influence of the hydrophobic effect) creates a curvature strain within the bilayer. If this strain is increased too far (e.g. by building up additional conformational disorder in the chain region by heating), eventually a phase transition will be induced, to a structure that allows the monolayer curvature to be expressed. In treating curvature, we must define both the mean curvature, H, and the Gaussian curvature, K, at each point on a chosen interface (which could be the centre plane of the bilayer, the polar/non-polar interface or some other suitable interface):

$$H = \frac{1}{2}(c_1 + c_2); \quad K = c_1 c_2, \tag{2}$$

where c_1 and c_2 are the principal curvatures at the given point on the interface. It is a well-established convention that, for a monolayer, negative mean curvature ($H < 0$) corresponds to curvature of the layer towards the water and away from the chain region, whereas positive mean curvature ($H > 0$) is the opposite. Helfrich [4, 5] developed the curvature elastic energy cost per unit area, g_c, of deforming a thin membrane layer as

$$g_c = 2\kappa(H - H_o)^2 + \kappa_G K, \tag{3}$$

where H_o is the spontaneous mean curvature; κ is the mean curvature (bending) modulus; and κ_G is the Gaussian curvature modulus.

The spontaneous mean curvature H_o is proportional to the *first moment* of the stress profile:

$$H_o = -\frac{1}{2\kappa}\int t(z) z dz. \tag{4}$$

H_o is expected to be *negative* for a monolayer of an amphiphile having a small, weakly hydrated headgroup and *positive* for an amphiphile with a large, strongly hydrated headgroup. Typical values for a range of lipids are tabulated in a recent review [6]. However, for a symmetric bilayer, the first moment will be zero by symmetry, and hence H_o (bilayer) $= 0$, even though H_o is not in general zero for the individual monolayers.

Helfrich also showed that the Gaussian curvature modulus κ_G is given by the second moment of the stress profile:

$$\kappa_G = \int t(z) z^2 dz. \tag{5}$$

For a monolayer, the origin of integration is taken at the *pivotal surface*, where the cross-sectional area does not change upon bending. This integral is then expected, usually, to be negative, $\kappa_G < 0$, meaning that a monolayer will prefer to curve into an elliptic shape (spherical or ellipsoidal), having positive Gaussian curvature. This favours micellar or inverse micellar phases based upon discontinuous packings of discrete aggregates. Typical values of the monolayer curvature moduli κ and κ_G for lipids are given in our recent review [3].

The value of κ_G for a bilayer is not simply twice the value of κ_G^m for a monolayer, but is given by the more complex expression

$$\kappa_G^b = 2\left(\kappa_G^m - 4\kappa^m H_o^m h\right), \tag{6}$$

where h is the distance from the centre of the bilayer to the pivotal surface. Thus for a bilayer, κ_G^b may be *positive*, if the lipid headgroups are sufficiently small and weakly repulsive/weakly polar, even when κ_G^m is negative. This tends to favour a saddle-surface deformation of the bilayer, which can only be stabilised by a topological transformation to a sponge-like bicontinuous phase (since the Gauss–Bonnet theorem states that the integrated Gaussian curvature of any surface is a constant, unless there is a change of topology). Such bicontinuous lyotropic phases will not be considered any further in the present review, but have been extensively discussed elsewhere (see [3, 7] and the references therein).

We note in passing that Alfred Saupe developed a curvature energy-based theory to explain the formation of tube-like myelin figures which are commonly observed in amphiphilic fluid lamellar phases which are in contact with water [8]. His explanation was based on the assumption that there is a spontaneous bilayer curvature induced by a concentration gradient across the lamellae. More recent treatments have found that the driving force is more likely to be interbilayer repulsion [9], with the characteristic coiling of the myelins being due to a small (approx 1 mN m^{-1}) net bilayer lateral tension [10].

1.2 Lyotropic phases and phase diagrams

In thinking about the various types of lyotropic liquid crystal phases, it is useful to consider a hypothetical phase map, where the various liquid-crystalline phases are arranged according to their average interfacial mean curvature, $<H>$ (see Figure 5). Parameters such as the water content, temperature, pressure, etc., tend to change the preferred mean curvature, $<H>$, and may induce transitions between different phases. It should be noted that a given real amphiphile system will only exhibit a subset of these phases. The flat lamellar bilayer phase, with $<H> = 0$, occupies a central location in this phase map.

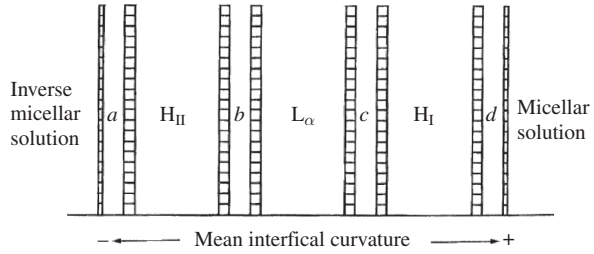

Figure 5. A hypothetical lyotropic phase map, showing the natural sequence of phases as a function of the average interfacial mean curvature. Taken, with permission, from Seddon *et al*. [7].

Moving to the right corresponds to the interfacial mean curvature becoming increasingly positive (the interface curving away from the water and towards the fluid hydrocarbon chain region). In region *c* bicontinuous phases, such as the bicontinuous cubic phases, are found. Beyond this the Type I hexagonal H_I phase, whose structure consists of a two-dimensional (2D) packing of indefinitely long cylindrical micelles, is found. In this phase the interface has a positive mean curvature, but a zero Gaussian curvature. Moving further right into region *d*, we find phases based on packings of discrete micellar aggregates. Such phases may be expected to be formed by amphiphiles which have large, strongly hydrated and/or charged headgroups, attached to relatively small hydrocarbon chain regions.

Moving leftwards from the lamellar phase, inverse bicontinuous phases are found in region *b*, followed by the inverse hexagonal H_{II} phase, consisting of a 2D hexagonal packing of indefinitely long inverse cylindrical micelles.

Curiously, various lipid systems undergo fluid lamellar–inverse bicontinuous cubic phase transitions *with increasing water content*, which is the opposite of what one would expect from these considerations. It has been suggested [3] that the additional water is not acting to tune the preferred curvature of the interface, which would be expected to *resist* inverse phase formation, but is instead inertly filling the aqueous regions of the cubic phases, allowing the already fully hydrated lipid interface to express its pre-existing preferred inverse interfacial curvature. In other words, the fluid lamellar phase is in a state of curvature frustration, which can be geometrically relaxed by adding additional water. Fredrickson and co-workers have developed a self-consistent field theory (SCFT) approach to calculating the temperature–composition phase diagram of weakly amphiphilic, hydrogen-bonding lipids such as the monoacylglycerol monoolein, and have thereby gained an understanding of the mechanisms underlying such anomalous phase sequences [11, 12]. In this course-grained SCFT approach, the monoolein headgroup can either have water bound to it (by hydrogen-bonding) or be unbound, depending on the water content and the temperature. The two amphiphile states have different headgroup volumes and different interactions with the chain region and the aqueous region of the phase. An interplay between hydrogen bond formation, headgroup volume and interactions, hydrocarbon chain splay (entropy) and the hydrophobic effect leads to the observed anomalous phase behaviour.

Moving further left into region *a* of Figure 5, to achieve a more negative interfacial curvature than in H_{II} implies that the inverse cylinders must break up into shorter inverse micellar aggregates, leading to phases based upon close packings of discrete inverse micelles.

1.3 Tuning interfacial curvature: hydration, T, p, addition of amphiphiles

As we have noted, for many single-chain surfactant systems, varying the hydration strongly changes the interfacial curvature, normally leading to phases of increasingly positive interfacial curvature with increasing water content. However, for various lipid systems with weakly polar headgroups, which tend to form inverse phases, hydration has a limited capacity to tune the phase behaviour, and instead variation of temperature and/or hydrostatic pressure are often more important. For example, for a range of fully hydrated dialkyl xylopyranosyl glycerols (double-chained glycolipids having a small, weakly polar xylose headgroup), it was possible to induce a transition from the H_{II} phase to an inverse micellar *Fd3m* cubic phase by heating [13]. The transition could be reversed by application of hydrostatic pressure [14]. Another study has found that a di-phytanyl chained glucolipid adopts the *Fd3m* phase over a wide range of temperature [15]. For phospholipid systems, the only way found so far of inducing the formation of ordered inverse micellar phases has been to incorporate into the phospholipid a weakly polar amphiphile with a small polar headgroup (see Figure 2), such as a diacylglycerol, a fatty acid or an long-chain alkanol [16].

1.4 Packing frustration and relaxing packing constraints

It should be recognised that the nature of the packing constraints are quite different between Type I and Type II ordered micellar phases. In the former, the aggregate dimensions are constrained by the requirement that no part of the hydrocarbon interior can be further away from the polar/non-polar interface than the length of a fully extended hydrocarbon chain. The

water forms the continuous region, but with no particular packing constraints other than the need to fill the volume with a uniform density. For a Type II phase, on the other hand, the continuous region is filled with fluid hydrocarbon chains and, since these are pinned at one end by the polar headgroups to the interface, no part of the continuous region can be further away from the interface than the length of a fully extended hydrocarbon chain (we are assuming at this point that no hydrophobic solutes have been added). There is no intrinsic constraint on the size of the water cores; however, they are not necessarily free to swell to a diameter that will relax the curvature of the amphiphile monolayer, as this will generate regions within the hydrophobic volume that are too far away from the interface to be reached by any of the hydrocarbon chains. A qualitative measure of the degree of chain packing frustration in inverse micellar phases may be obtained from the *packing fraction*, assuming the aggregates to be regularly shaped solids. Thus, since circular cylinders in a close-packed 2D hexagonal lattice have a packing fraction of 0.91, this implies that 9% of the hydrophobic volume in the inverse hexagonal H_{II} phase is potential void volume, which needs to be filled by some of the hydrocarbon chains deviating away from their preferred conformational state (see Figure 6). Note that an additional mechanism to relieve the packing frustration could be a deformation of the polar/non-polar interface from a circular to a hexagon shape.

A chain-stretching model has been developed to quantify the chain packing frustration in densely-packed phases of polystyrene (PS) colloidal polymeric particles mixed with polystyrene-poly(2-vinylpyridine)

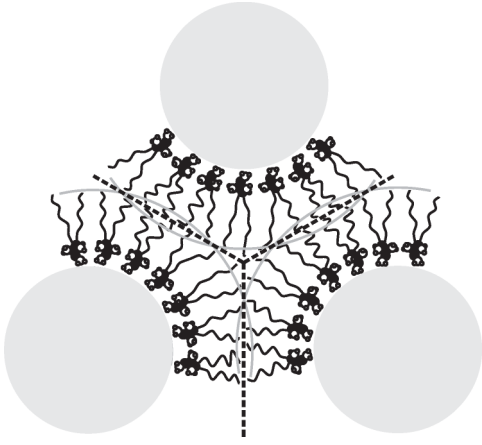

Figure 6. Chain packing frustration within the H_{II} phase, due to the need for hydrocarbon chains to stretch or compress away from their preferred conformational length, in order to fill uniformly the hydrophobic volume of the phase. Taken, with permission, from Shearman *et al.* [3].

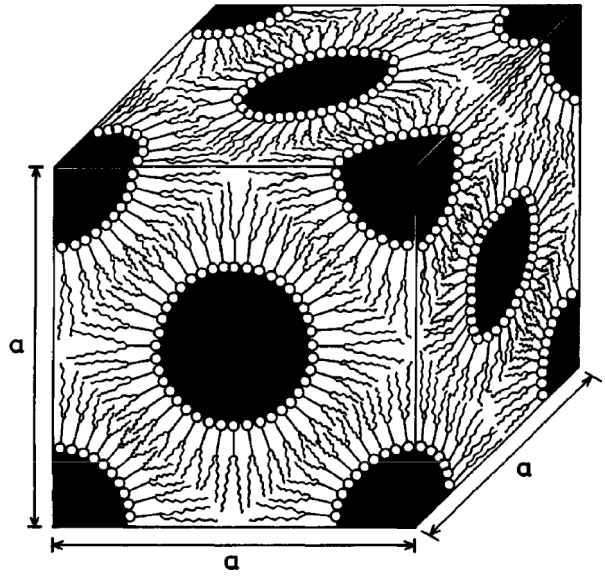

Figure 7. A hypothetical fcc phase of spherical inverse micelles, showing the severe problem of uniformly filling the hydrophobic volume of the phase with the hydrocarbon chains of the amphiphile. Taken, with permission, from Murakami *et al.* [18].

(PS-PVP) block copolymers [17]. It was shown by solving analytically for a 2D hexagonally-packed colloid system that the PS/PVP interface deforms from circular to hexagonally-faceted, in order to reduce the PVP chain packing frustration pressure.

The chain packing frustration becomes much more severe for 3D close packings of inverse micelles (see Table 1). To illustrate this, consider a hypothetical face-centred cubic (fcc) packing of inverse spherical micelles, as shown in Figure 7.

The potential void volume of such an fcc phase would be 26% of the unit cell, and this would create such a large amount of chain packing frustration that such phases are not normally observed experimentally.

However, more complex structures have been observed, most commonly an inverse micellar cubic phase of spacegroup *Fd3m*, which consists of two

Table 1. Packing fractions for various close packings of spheres.

Close-packed phase	Packing fraction
Pm3m (sc)	0.524
Im3m (bcc)	0.680
Fd3m	0.710
Fm3m (fcc)	0.740
$P6_3/mmc$ (hcp)	0.740
p6m (2D hexagonal)	0.907

types of quasi-spherical inverse micelle, of different diameters. Curiously, the potential void volume is 29%, worse than for an fcc packing of uniform spheres. However, it turns out that the *variation in distance* from the interface to the centre points of the hydrophobic regions are much reduced for the *Fd3m* packing, leading to a smaller chain-stretching free energy cost [19]. For monoglycerides such as monoolein or monolinolein, the *Fd3m* phase can be induced by addition of alkanes [20] or other hydrocarbon solutes such as limonene to relax the packing constraints [21–24].

2. Ordered micellar and inverse micellar phases

Ordered normal or Type I micellar lyotropic phases, existing between the isotropic micellar solution and the hexagonal liquid crystalline phase, have been reported since the 1960s and these have been denoted as I_1 phases, due to their being optically isotropic. The ordered inverse or Type II micellar phases, with their location in the expected sequence of lyotropic phases essentially mirroring that of the ordered micellar phases, are a more recent phenomenon. In 1990, a detailed list of surfactant/water and surfactant-like/water systems displaying discontinuous or bicontinuous cubic phases was compiled by Krister Fontell [25] and will not be duplicated here.

Five Type I ordered micellar lyotropic phases, with 3D packings, have so far been observed. All but one of these structures are cubic, with the remaining one adopting a 3D hexagonal close packed (hcp) packing. X-ray diffraction is generally used for the crystallographic identification and structural analysis of lyotropic phases (see Figure 8), whereas freeze-fracture electron microscopy (FFEM) is a complementary technique used for the direct visualisation of the real-space structure.

Table 2. Allowed Bragg reflections of the ordered micellar and inverse micellar phases.

Mesophase	Spacegroup Number	Observed for: Type I	Observed for: Type II	Bragg reflections
Pm3n	223	✓		$\sqrt{2}$, $\sqrt{4}$, $\sqrt{5}$, $\sqrt{6}$, $\sqrt{8}$...
Fm3m	225	✓		$\sqrt{3}$, $\sqrt{4}$, $\sqrt{8}$, $\sqrt{11}$, $\sqrt{12}$, $\sqrt{16}$...
Im3m	229	✓		$\sqrt{2}$, $\sqrt{4}$, $\sqrt{6}$, $\sqrt{8}$, $\sqrt{10}$...
Fd3m	227	✓	✓	$\sqrt{3}$, $\sqrt{8}$, $\sqrt{11}$, $\sqrt{12}$, $\sqrt{16}$, $\sqrt{19}$...
$P6_3/mmc$	194	✓	✓	$\sqrt{(4/3)}$, $\sqrt{(3/2)}$, $\sqrt{(41/24)}$, $\sqrt{(17/6)}$...
$P4_332$	212		✓	$\sqrt{2}$, $\sqrt{3}$, $\sqrt{5}$, $\sqrt{6}$, $\sqrt{8}$, $\sqrt{9}$, $\sqrt{10}$...

The allowed Bragg reflections for the various ordered micellar phases are listed in Table 2.

The most common ordered micellar phase is the *Pm3n* (Q^{223}) phase, observed in numerous non-ionic and ionic surfactant–water systems as well as in certain lipid/water systems. Two different structures have been proposed for this phase, where in the first model the unit cell is composed of eight identical, slightly elongated micelles, two rotating isotropically and six rotating around a short axis [27]. In the second model, there are two quasi-spherical micelles and six disk shaped micelles per unit cell, as illustrated in Figure 9(a) [28, 29]. The fcc *Fd3m* phase was also found to be formed by two types of micelles, but

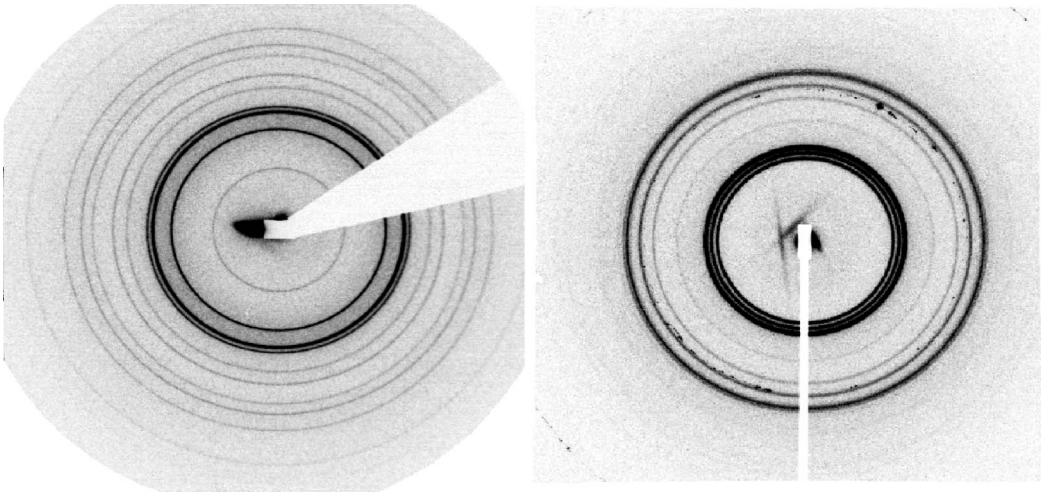

Figure 8. Typical small-angle X-ray patterns of ordered inverse micellar phases: (a) the *Fd3m* cubic phase (unpublished data), and (b) the *$P6_3/mmc$* 3D hexagonal phase (taken, with permission, from Shearman *et al.* [26]).

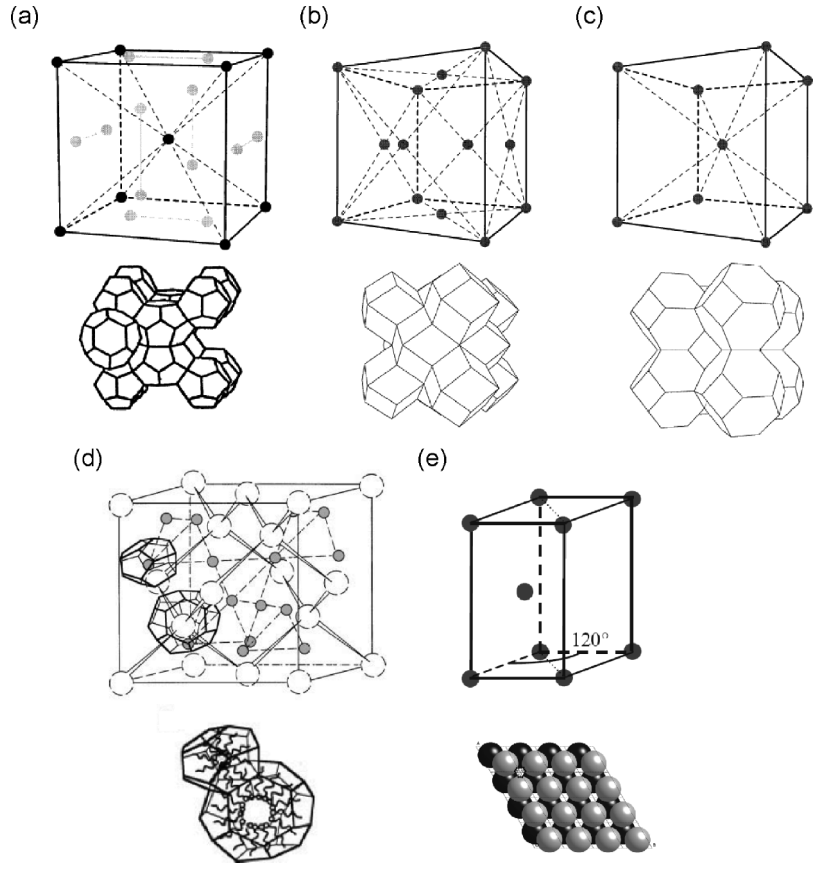

Figure 9. The packing of the ordered micellar phases: (a) *Pm3n*, (b) *Fm3m*, (c) *Im3m*, (d) *Fd3m,* (e) *P6$_3$/mmc*. The first three (taken, with permission, from Sakya *et al.* [32]) are Type I structures, whereas the latter two are shown as Type II, inverse micellar phases (taken, with permission, from Seddon *et al.* [16] and Shearman *et al.* [26], respectively).

in this case the shape of both of the micelles was found to be quasi-spherical, as shown in Figure 9(d) [30]. Unlike the *Fd3m* phase, the *Fm3m, Im3m* and *P6$_3$/mmc* phases all consist of identical quasi-spherical micelles, packed onto fcc, body-centred cubic (bcc) and hcp lattices respectively, as shown in Figure 9(b), (c) and (e). It is interesting to note that the only difference between the fcc and hcp lattices are their stacking sequences (ABCABC and ABABAB, respectively) along the body-diagonal (111) direction, resulting in only a minimal free energy difference between the two phases. Finally, the *P4$_3$32* phase is formed from one 3D continuous network of water channels (similar to those found in the bicontinuous cubic *Ia3d* phase) that co-exists with inverse micellar globules, believed to be composed of a lipid monolayer enclosing an inner protein core [31].

We note that there is a close structural relationship [33, 34] between the *Pm3n* and *Fd3m* cubic phases, and respectively the A15 and C15 tetrahedrally close-packed (tcp) networks found in ordered foam packings, as well as the well-known cubic clathrate hydrates of space groups *Pm3n* and *Fd3m*.

2.1 Type I ordered micellar phases

2.1.1 Non-ionic surfactant/water and surfactant-like/water systems

2.1.1.1 Polyoxyethylene surfactants. Polyoxyethylene surfactants are typical non-ionic surfactants, forming micelles in water above the critical micelle concentration, and at high enough surfactant concentrations, various liquid crystalline phases are generally observed, apart from those polyoxyethylene surfactants with an alkyl chain length of fewer than eight carbon atoms. A systematic study of poly(oxyethylene) alkyl ethers ($C_nH_{2n+1}(OCH_2CH_2)_mOH$; C_nEO_m) in water revealed that micellar cubic phases were formed for $m \geq 8$ [35]. Interestingly, the temperature at which the micellar cubic phases underwent a phase transition into a micellar solution was found to be strongly dependent on the size of the hydrophilic region, becoming increasingly more stable with increasing EO number, but independent of the alkyl chain length. Combined with the observation that the ordered micellar phases were generally found at both low temperatures and low surfactant concentrations, these findings were concluded to be due to the effective

cross-sectional area of the polar headgroup, with low temperatures, low surfactant concentrations and high EO numbers all causing the headgroup area to increase. The headgroup area is directly related to the curvature of the aggregate (micelle) surface; a smaller headgroup area results in a larger radius of curvature, i.e. becoming less curved, which destabilises the aggregate causing the ordered micellar phases to be less favoured.

Although for the majority of binary polyoxyethylene surfactant/water systems the ordered micellar phases are believed to be either *Pm3n* or *Fm3m*, recent developments have revealed a more complex phase behaviour for some of these surfactants. The first example of a 3D hcp $P6_3/mmc$ phase existing in a lyotropic system was found in the polyoxyethylene surfactant $C_{12}EO_8$/water system [36]. Subsequent detailed analysis of the reconstructed electron density map has shown that the micelles comprising the phase are perfectly spherical (see Figure 10), each with a low-density core formed by the hydrophobic alkyl chains together with a high-density shell of oxyethylene groups, and with an aggregation number estimated to be 96 [37]. As with other Type I ordered micellar phases, the regions between the micelles are filled with water.

Multiple micellar cubic phases have also been reported for binary polyoxyethylene surfactant/water systems, with $C_{12}EO_{12}$ displaying no fewer than three such phases [32]. Figure 11 shows the temperature–composition phase diagram for this system, with the

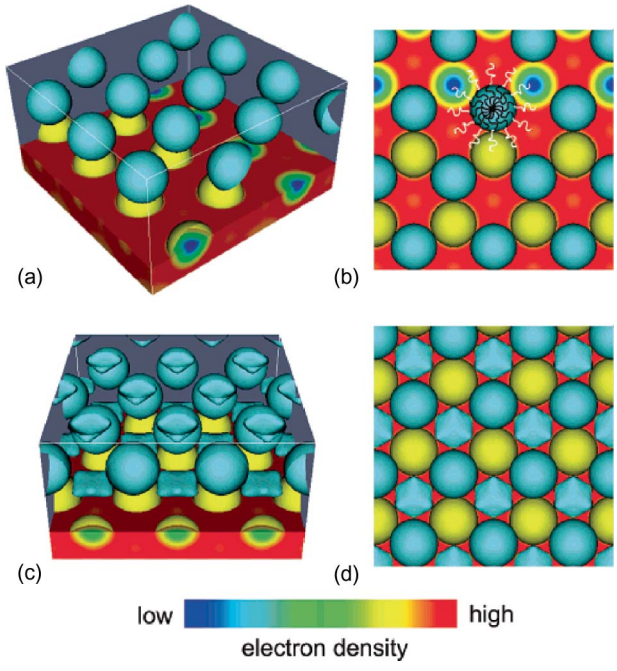

Figure 10. Electron density maps for the Type I $P6_3/mmc$ phase of $C_{12}EO_8$/water (taken, with permission, from Zeng *et al.* [37]).

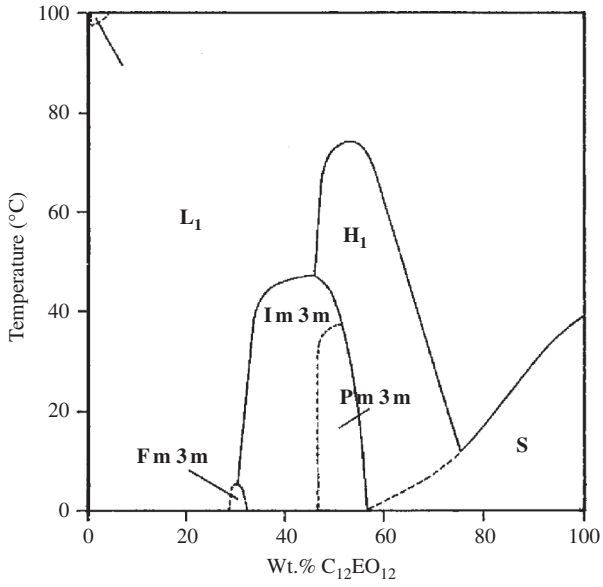

Figure 11. The temperature–composition phase diagram of $C_{12}EO_{12}$/water. Taken, with permission, from Sakya *et al.* [32].

phase sequence *Fm3m* →*Im3m* → *Pm3n* with decreasing water content. The aggregation numbers of the micelles in these phases are in the region of 80. The transition between the *Im3m* and *Pm3n* phases was found to occur by a rearrangement and deformation of micelles rather than any fusion or fission events, suggesting that a low-energy transition pathway exists between these two phases.

By tuning the system, it has been found that the region over which ordered micellar phases are seen can be extended or reduced considerably. Methods include the addition of a third component to binary polyoxyethylene systems as well as the modification of either the aliphatic chain region or the hydrophilic headgroup of the surfactant. The binary $C_{12}EO_{25}$/water system has been examined with regard to the former method, with the addition of various different oils, ranging from linear and branched alkanes and alkenes, through to polyols and perfumes [38–40]. Shorter-chain hydrophobic oils were found to increase the thermal stability of the micellar cubic phase, whereas amphiphilic oils had the reverse effect; these two phenomena are believed to be caused by opposing effects on the curvature due to the difference in location within the micelle, with the hydrophobic oils forming a reservoir in the centre of the micelle and the amphiphilic oils residing at the polar–non-polar interface. Changing the nature of the surfactant itself has also been demonstrated to have a significant effect, with both the replacement of the linear carbon chain in C_nEO_{30} surfactant/water systems with cholesterol [40], and branching of the hydrophilic chain [41], causing the micellar cubic phase to be stabilised.

2.1.1.2 Amphiphilic block copolymers. In general, amphiphilic block copolymer/water systems have many similarities to polyoxyethylene surfactant/water systems, but with some disparities (excluding the ultra-long polyoxyethylene surfactant/water systems, that behave as copolymers [42]). Such systems consist of a number (two or greater) of different homopolymers covalently bonded together to form 'blocks' that have different hydrophilicities. Such blocks can include polyoxyethylene, polyoxypropylene, polystyrene, polyoxybutylene or polyisoprene. A typical amphiphilic diblock copolymer may consist of a polyoxyethylene and a polyoxypropylene block, where the latter would be the block with a higher hydrophobicity, i.e. water is able to solvate the polyoxyethylene block but is a relatively poor solvent for polyoxypropylene. The phase behaviour of block copolymer/water systems is dictated not only by their composition, for example, their compositional asymmetry and architecture, i.e. the type of block, but also by their molecular weight. This last factor is crucial as the desire for the individual blocks to segregate increases with increasing molecular weight, and thus only at a certain minimum limit will ordered structures and liquid crystalline phases be seen [43]. However, a well-chosen block copolymer system can reveal a multitude of liquid crystalline phases, ranging from highly positively curved species such as Type I micellar cubics, hexagonal and bicontinuous cubic phases through to highly negatively curved phases [44, 45]. Ordered micellar phases are generally observed for high molecular weight block copolymers with a relatively large hydrophilic region. For typical solvated block copolymers such as polyoxyethylene–polyoxybutylene/water systems, the structure of the ordered micellar phase can also be tuned simply by altering the composition. By varying the asymmetry of the block copolymer, Hamley *et al.* [46] found that fcc-packed micellar cubic phases were formed for those block copolymers with a short hydrophilic block, and bcc-packed phases formed for long hydrophilic blocks, as shown in Figure 12. They concluded that this was due to the change in nature of the micelle, with the micelle acting as a hard sphere with a short-range intermolecular potential for the former case and a soft sphere with a longer-range potential for the latter.

However, fcc and bcc packings are not the only ordered micellar structures observed for block copolymers, with a second example of the rare Type I hcp $P6_3/mmc$ phase seen for the poly(oxyethylene)–polyoxypropylene–polyoxyethylene triblock copolymer $(EO)_{20}(PO)_{70}(EO)_{20}$ ($((OCH_2CH_2)_m(OCH(CH_3)CH_2)_n(OCH_2CH_2)_m$ with $m = 20$ and $n = 70$) when mixed with ethanol and water [47]. By tuning the amount of ethanol, the $P6_3/mmc$ phase either exists on its own or

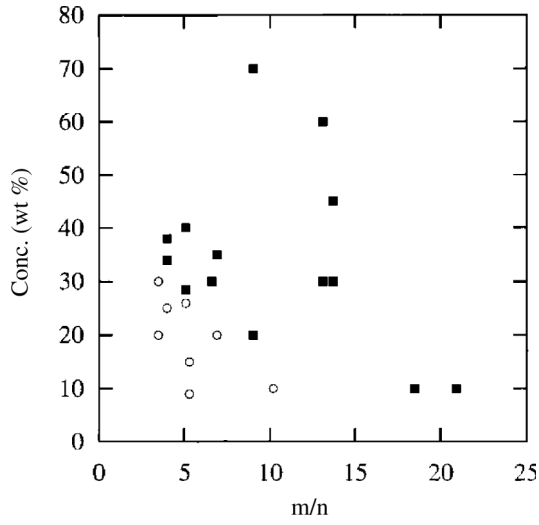

Figure 12. Phase diagram showing the regions of stability for the two different ordered micellar cubic phases formed by polyoxyethylene–polyoxybutylene diblock copolymers in water, where *m*/*n* represents the ratio of the number of oxyethylene units to oxybutylene units, and the empty circles and filled squares symbolise the fcc and bcc phases, respectively. Taken, with permission, from Hamley *et al.* [46].

coexists with the fcc-packed *Fm3m* phase, but the addition of large quantities of ethanol was found to drive the block copolymer system eventually into an isotropic micellar solution (L_I) since an increased ethanol concentration induced smaller micelles (and hence lower aggregation numbers).

Finally, one unique characteristic of solvated diblock copolymers for which at least one of the blocks is polyoxyethylene is their temperature dependence, where for certain copolymer concentrations the high-temperature L_I phase is found to convert on cooling first to an ordered micellar cubic phase and then to a re-entrant L_I phase [48, 49]. At the high temperature boundary, decreasing the temperature causes the solvent to be less poor, which, together with the fact that polyoxyethylene has a negative coefficient of solubility in water, causes an increase of equivalent hard-sphere radii of the micelles, at which point an ordered micellar cubic phase is formed [50]. However, at the low-temperature boundary the L_I phase is formed again due to the volume fraction of spheres (i.e. micelles) not reaching a critical close-packed limit.

2.1.1.3 Other non-ionic surfactants. Other examples of non-ionic surfactants that form ordered micellar phases include sugar-based surfactants such as disaccharides. However, the stereochemistry of such surfactants influences the phase behaviour: α-N dodecyl-D-maltoside forms both *Im3m* and *Pm3n* micellar cubic phases, and yet the β-anomer, β-N dodecyl-D-maltoside, forms no ordered micellar

phases [51, 52]. The configuration of the anomeric carbon is not the only influence on the likelihood of formation of ordered micellar phases; molecules with bulky, polarised or kinked linkages between the hydrophobic chain regions and the sugar headgroups are also more likely to form such phases, since the interface will be more positively curved (which results in the packing parameter, *P*, being reduced) [52].

2.1.2 *Ionic surfactant/water and surfactant-like/water systems*

2.1.2.1 Monovalent surfactants. Type I ordered micellar lyotropic phases have been reported for both cationic and anionic monovalent surfactants. One such cationic surfactant that has been shown to form the *Pm3n* phase in water is dodecyltrimethylammonium chloride [27, 53]. Extending or shortening the alkyl chain length by more than two carbon atoms, however, causes the *Pm3n* phase to disappear [54]. For the former case, it is believed that an increase in alkyl chain conformations causes the interfacial curvature to be reduced, increasing the size of the micelles and therefore destabilising the micellar cubic phase; any effect due to counterion binding is considered to be minimal, as this same effect has also been observed for zwitterionic surfactants [55]. For the latter case of chain-shortening, several contributing factors caused by the smaller micelle size, such as increased entropy, may cause the change in phase behaviour [55]. Finally, changing the chloride counterion to either bromide or iodide has a similar effect to over-lengthening or shortening the hydrophobic chain, with an increase in the counterion binding destabilising the *Pm3n* phase for the dodecyltrimethylammonium halide/water system. Finally, reflecting the observations made for polyoxyethylene surfactant/water systems, the addition of an extra component, for example a hydrophobic oil, to a binary cationic surfactant/water system that forms an ordered micellar phase will promote its stability [56].

Hydrated anionic surfactant systems tend only to form Type I micellar cubic phases when extra constituents are added, as evidenced by the multi-component system sodium dodecyl sulphate/butanol/toluene/salt (NaCl)/water, which uniquely forms both ordered micellar cubic *Fd3m* and *Pm3n* phases; this system is so far unique in being the only example of the *Fd3m* phase seen for a Type I system (as confirmed by self-diffusion measurements), and the lattice parameters are surprisingly large [34, 57].

2.1.2.2 Divalent surfactants. By examination of a number of different divalent cationic and anionic surfactant/water systems [58, 59], Hagslätt *et al.* have proposed that the formation of micellar cubic phases is a general feature of all divalent surfactant/water phase diagrams [59]. Although this universal theory should, in truth, be confined to relatively narrow bounds such as monoalkyl divalent surfactants with a medium-long alkyl chain length, this proposal has been corroborated by some anionic *N*-lauroyl-L-glutamate/water systems [60], with the micellar cubic region found in all these divalent surfactant/water systems being of *Pm3n* symmetry and stable over a wide range of surfactant concentrations. The occurrence of this stable micellar cubic phase for divalent surfactant/water systems is believed to be caused by the suppression of any micellar growth usually seen with increasing surfactant concentration for monovalent surfactants, which is likely to be due to the high charge density at the headgroups inducing a highly positive interfacial curvature [59]. Mixtures of charged surfactants have also been shown to produce Type I micellar cubic phases, with their formation being promoted by high surface charge densities [61].

2.1.3 *Lipid/water and lipid-containing/water systems*

The best-known group of lipids that, in conjunction with water, will form ordered Type I micellar phases are the saturated lysophospholipids [62–66]. Although relatively scarce, with fewer than one phospholipid in 20 found in a typical cell being a lysophospholipid, they have been shown to play a major role in several signalling pathways, membrane fission and many other biological processes (see, e.g., [67, 68]). Their ability to self-aggregate into micelles at low phospholipid concentrations, which then coalesce further into ordered phases at higher concentrations, is due to their inherently high solubility compared with those of their parent di-chained phospholipids. Peculiarly, although both saturated and unsaturated lysophosphocholines form Type I micelles, the unsaturated species are unable to form ordered micellar phases due to the diffuse, polydisperse nature of the micelles [64]. The micellar cubic phase formed by egg-phosphatidylcholine and several saturated lysophosphatidylcholines ($C_n$lysoPC where n = 12–16) has been identified as *Pm3n*, the most common of the Type I ordered micellar phases [27, 28]. The micellar cubic phase can be formed in excess aqueous solution by addition of polyethylene glycol to the water [69].

Lastly, ganglioside/water systems have also been found to form a number of ordered Type I micellar cubic phases, with *Pm3n*, *Im3m* and *Fm3m* all being seen [70]. These Type I micellar cubics are formed due to the large effective size of the headgroups, resulting in a desire to form highly positively curved lyotropic phases. An example of a ganglioside with only one long-chain, atypical of most gangliosides, is shown in Figure 13 and was found to form both *Pm3n* and *Fm3m* phases.

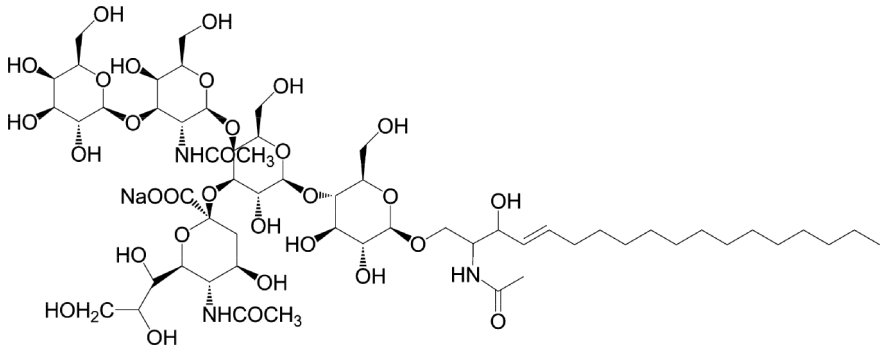

Figure 13. The chemical structure of a GM1 (acetyl) ganglioside, emphasising the large size of its hydrophilic headgroup region, corresponding to a packing parameter $P \ll 1$.

2.2 Type II inverse ordered micellar phases

Although phases based upon ordered packings of inverse micelles had been proposed in the past, by the late 1980s the consensus view was emerging that such phases do not exist [25, 71]. A cubic phase of spacegroup *Fd3m* had been observed in a lipid extract from *Pseudomonas fluorescens* [72], but its structure was unknown at that time. Later, the same phase was observed in a number of lipid systems [73], and a hybrid continuous/inverse micellar structure was proposed. Around the same time, the *Fd3m* phase was identified in a dioleoyl phosphatidylcholine (DOPC)/dioleoylglycerol (DOG) mixture, and it was proposed that it might have a structure based on an *Fd3m* packing of two types of inverse micellar aggregates [74]. This suggestion was stimulated by the theoretical/geometrical work of Charvolin and Sadoc, who proposed that an *Fd3m* packing of discrete micelles should be a favourable packing [33]. This is now the generally accepted structure for this phase [75], and this has been confirmed by a FFEM study [30].

The Type II *Fd3m* phase has since been reported for many other binary lipid systems in water, such as phospholipid/diacylglycerol [75–77], phosphatidylcholine/fatty alcohol [78], monoolein/oleic acid and dimyristoylphosphatidylcholine/myristic acid [31, 73, 76]. It should be noted that hydrated oleic acid/sodium oleate mixtures are also known to form the *Fd3m* phase [79], as are mixtures of oleic acid with the cationic phospholipid dioleoylethylphosphatidylcholine (EDOPC), which is widely regarded as a possible transfection agent [80]. For a hydrated mixture of phosphatidylcholine/phosphatidylethanolamine/cholesterol in a molar ratio of 2:1:1, the inverse bicontinuous *Pn3m* cubic phase was transformed to an *Fd3m* inverse micellar cubic phase by addition of diacylglycerol in excess of 30 mol% [81].

The fact that the *Fd3m* phase was usually observed in hydrated binary lipid systems, led to the suggestion that two lipid components of differing amphiphilicities were required in order to stabilise the two inverse micelles of different diameters (and hence different curvatures), and hence allow the ordered micellar phase to form. However, a number of single lipid/water systems have now disproved this notion, with glycolipids such as the 1,2-di-*O*-alkyl-3-*O*-(α-or-β-D-xylopyranosyl)-*sn*-glycerols with chainlengths greater than C14 [13], and 1,3-di-*O*-phytanyl-2-*O*-(β-glucosyl)glycerols [15, 82] all able to form the *Fd3m* phase over a wide range of water concentrations and temperatures. However, glycolipids with short, unbranched chains or more than one sugar ring are unable to form the *Fd3m* phase as a sufficiently negative interfacial curvature needed for such an ordered micellar phase is not achievable. It is still unclear, for binary lipid/water systems, why certain glycolipids can form the *Fd3m* phase but phospholipids apparently cannot. One possible hypothesis is that the single sugar ring may be able to adopt two different conformations, changing its effective hydrophilicity, and hence the preferred interfacial curvature.

Although the *Fd3m* phase has been most often observed for lipid/water systems [74, 75, 77], the *Fd3m* phase has also been reported for a number of other amphiphiles such as block copolymers. For these, the addition of both water and oil (causing the solubilisation of both the hydrophilic and hydrophobic blocks) allows the formation of inverse micellar cubic phases at high surfactant concentrations [44, 83]. In fact, additives such as oils can also be used to drive less highly negatively curved mesophases formed by lipids into the *Fd3m* phase as mentioned in Section 1.4 [21–24], as they partition into the hydrophobic region, which in turn reduces the packing frustration.

Recently, a second ordered inverse micellar phase has been reported. Unlike the *Fd3m* phase it was determined to be of 3D hexagonal packing; such a packing had been intimated previously for a mixture of DOPC/DOG (with a DOG weight percentage of 60%) below limiting hydration, but had not been

identified due to the paucity of Bragg reflections [16]. However, it was found that, by doping DOPC/DOG with a small molar ratio of cholesterol, the phase was stabilised in excess water and it was finally identified as a 3D hexagonal inverse micellar phase of the space group $P6_3/mmc$ [26]. As with its Type I counterpart, the ratio of the lattice parameters of the 3D hexagonal unit cell ($c/a = 1.629$) revealed that the packing of the quasi-spherical inverse micelles was hexagonal close-packed (for ideal hcp packing, $c/a = 1.633$).

Finally, the only known example of the hybrid inverse micellar/bicontinuous $P4_332$ phase was identified for a hydrated mixture of monoolein and the water-soluble protein cytochrome C. The binary monoolein/water system forms an inverse bicontinuous cubic phase, but the addition of the protein drives it into the $P4_332$ phase, an effect caused by the favourable interaction between the charged proteins and the lipids inducing a more negative interfacial curvature [31, 84]. The adoption of the $P4_332$ phase, however, is not universal for lipid–protein mixtures in water and presumably requires a matching of the relative sizes of the protein and the water.

3. Properties of ordered micellar phases

3.1 Epitaxy

Geometric and orientational relationships have sometimes been identified for two liquid crystalline phases in thermodynamic equilibrium undergoing a transition from one to the other and this has also been postulated for micellar ordered phases, specifically regarding both the epitaxial relationships between the micellar ordered phases and the neighbouring hexagonal phase and those between the ordered micellar phases themselves. Determining such relationships is extremely useful as they may give insight into possible low-energy kinetic pathways and transition mechanisms. However, although comparisons of the spacings between planes, such as the (10) hexagonal planes, for each of the phases involved in the transition may suggest an epitaxial relationship, only by studying aligned samples (or a monodomain) can this be positively confirmed. Such a study has been carried out for the transition $H_I \leftrightarrow Im3m$ for the non-ionic surfactant $C_{12}EO_{12}$/water system, where an epitaxial relationship relating the direction of the hexagonal cylinders to the [111] direction of the $Im3m$ plane was found, as shown in Figure 14 [32].

An epitaxial relationship for the $H_I \rightarrow Pm3n$ transition has also been suggested for a number of different surfactant/water systems, with the (10) planes of the hexagonal phase transforming into the (211) planes of the $Pm3n$ phase [52, 56, 85, 86], a conclusion reached from the spacings of their Bragg peaks, but which has been contested [32].

Finally, although somewhat outside the scope of this review, it is interesting to note that epitaxial relationships have been reported for the fcc $\leftrightarrow$ bcc, hcp $\leftrightarrow$ bcc, hcp $\leftrightarrow$ H_I and bcc $\leftrightarrow$ H_I transitions observed in certain block copolymer solutions where the solvent is a polystyrene or polyisoprene selective solvent rather than water [87–89].

3.2 Self-diffusion and electrical conductivity

The unique structural properties that Type I and Type II ordered micellar phases possess allow their identification by a number of techniques. Small-angle X-ray diffraction (SAXS) is generally used to determine the symmetry of the lyotropic phase, but cannot readily identify the continuity of a cubic phase, i.e. whether the lyotropic phase is a discontinuous ordered micellar or a bicontinuous cubic phase, unless sufficiently high-resolution electron density maps can be obtained. A second technique must, therefore, be used in conjunction with SAXS to distinguish the phase unequivocally. The Type I micellar cubic phases have

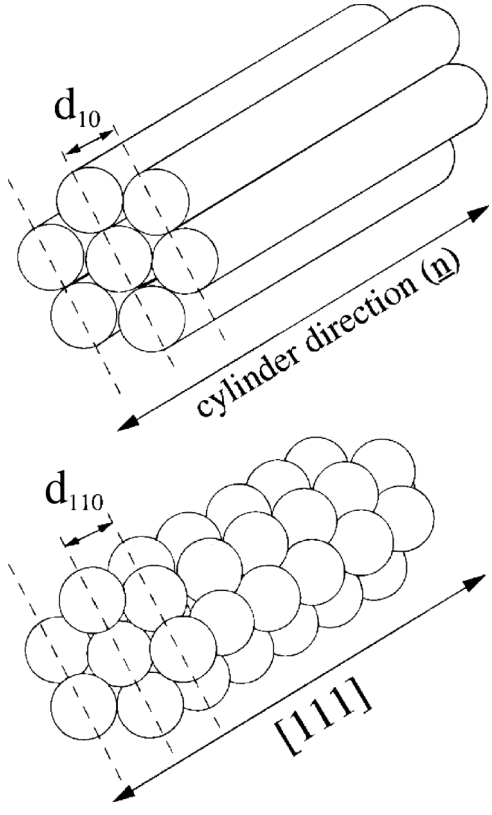

Figure 14. Epitaxial relationship between the 2D hexagonal H_I and $Im3m$ micellar cubic phases of the polyoxyethylene surfactant $C_{12}EO_{12}$/water system, taken, with permission, from Sakya *et al.* [32].

sometimes been named 'ringing gels' [90, 91], since they ring when tapped with a soft object. However, it has been reported that this phenomenon is not actually unique to these phases [25] and self-diffusion and electrical conductivity offer other, more reliable, methods of identification.

For binary amphiphile/water mixtures, self-diffusion measurements can be carried out on either of the two components, with ^{1}H pulsed field gradient nuclear magnetic resonance being the standard technique used to determine self-diffusion coefficients. For Type I ordered micellar phases, where amphiphilic micelles possessing a hydrophobic core are surrounded by water, it would be expected that the water would be able to diffuse easily across long distances but the amphiphiles would diffuse slowly. The Type I bicontinuous cubic phases would be expected to exhibit much larger diffusion coefficients, since the amphiphile mobility is expected to be far greater in a continuous rather than a discontinuous structure [92]. These two hypotheses have been confirmed by numerous studies (see [93, 94] for exhaustive lists), but one such example that can be used to illustrate this is the ternary $C_{12}EO_5$/decane/water system, where the self-diffusion coefficients for both the non-ionic surfactant and the hydrophobic oil, located within the micelles of the micellar cubic *Pm3n* phase were found to be slow and of the same order of magnitude ($\sim 10^{-13}$ m^2 s^{-1}), whereas the self-diffusion of the water was found to be approximately the same as that of free water ($\sim 10^{-9}$ m^2 s^{-1}) [95]. Translational self-diffusion coefficients of comparable orders of magnitude have been reported for the *Pm3n* phase formed by the cationic surfactant dodecyltrimethyl ammonium chloride, at high water contents [92, 96]. Above a certain surfactant concentration, the surfactant self-diffusion coefficient of this system then increases by a factor of 10 due to the system adopting a bicontinuous cubic phase. The self-diffusion of water within Type II bicontinuous cubic phases has been found to be similar to those of their counterparts, the Type I bicontinuous cubic structures ($\sim 10^{-10}$ m^2 s^{-1}) [93, 94], although amphiphile self-diffusion coefficients cannot be so easily compared (broadly speaking, the diffusion coefficients for phospholipids forming bicontinuous cubic phases are around 10^{-12} m^2 s^{-1} but those of simple single-chain amphiphiles can be significantly higher); however, the Type II micellar cubic *Fd3m* phase has revealed some unexpected findings. Initial studies by Hendrikx *et al.* [97] found that the amphiphile translational self-diffusion coefficients of the *Fd3m* phase for two different ternary systems were faster than expected and of a similar order of magnitude to those reported for inverse bicontinuous cubic phases, but that the water self-diffusion was about two orders of magnitude lower, consistent with discrete water regions. These results were corroborated by Orädd *et al.* [75] who also observed a slow translational diffusion coefficient for DOPC, one of the amphiphiles in the ternary DOPC/DOG/water system, but a faster self-diffusion coefficient for DOG. These observations led to the conclusion that such a system comprised inverse micelles formed mostly by the phospholipid, which enclosed water, surrounded by a continuous matrix of DOG. Although a technique frequently used for the determination of the structure of a cubic phase, it must be noted that the self-diffusion coefficients of the components, for example water, are highly dependent on a range of factors including the temperature of the system [75] and, therefore, should be viewed with some caution. Finally, an alternative approach to discriminate between the normal and reverse discontinuous and bicontinuous cubic phases has been developed, by studying the rate at which the phase is dyed after the addition of either an oil- or a water-soluble dye to the lyotropic phase [98].

Electrical conductivity measurements have been used for many years as a simple way of identifying not only the cmc of surfactants but also their lyotropic liquid crystalline mesophases and associated phase transitions (see, e.g., [99, 100]). Notably, Alfred Saupe and his co-worker Panos Photinos carried out numerous studies into the electrical conductivity of lyotropic phases, as well as calculations of this property for hexagonal, nematic and defective lamellar phases [101–109]. Electrical conductivity essentially examines the mobility of ions through any material, and can, therefore, be used to distinguish water continuous phases from water discontinuous phases. Uncharged systems are frequently doped with small amounts of salt to aid measurements although it should be noted that this in itself can alter the phase behaviour of a lyotropic system. From the difference in nature of the inverse micellar cubic *Fd3m* and the inverse bicontinuous cubic *Pn3m* phases, the conductivity of the *Fd3m* phase would be expected to be far lower and in fact this has been reported to be the case, with the conductivity of the bicontinuous phase being three orders of magnitude higher [16].

Several other complementary methods have also been used in order to identify whether a cubic phase is bicontinuous or discontinuous. These range from FRAP (fluorescence recovery after photobleaching) [110] and modulated fringe pattern photobleaching [111] to FFEM [30]. Both of the fluorescence techniques suffer from the intrinsic problem that they require a fluorescently labelled molecule in order to determine diffusion rates. Unfortunately, these rates have been found to depend on the hydrophilicity of the

fluorescent probe to a certain degree [112], and, therefore, any conclusions drawn cannot necessarily be considered substantive.

4. Conclusions

Apart from their inherent academic interest in the field of soft matter self-assembly, ordered micellar and inverse micellar lyotropic phases have a number of unique features which may render them useful for a wide range of applications. Cubic and 3D hexagonal micellar phases have been used for templating mesoporous materials [113–115] and as carriers for optical chemosensors [116]. Ordered inverse micellar phases such as *Fd3m* and $P6_3/mmc$ have the key property that they are stable in excess aqueous solution, which is very important for potential biological or biomedical applications. The 3D hexagonal phase $P6_3/mmc$ is the only known self-assembled lyotropic phase whose structure consists of a periodic close packing of identical inverse micelles. Such phases could have wide-ranging uses such as the storage and slow controlled release of drugs, with precise pharmacokinetics, or as nanoreactors, where the chemical or biochemical reactions would take place in identical spherical aqueous compartments having volumes as small as 10^{-4} attoliters (10^{-22} litres). They could also be used to form periodic 3D lattices of encapsulated nanoparticles, separated from each other by a low permittivity, 20–30 Å thick, fluid hydrocarbon region, which might have interesting optoelectronic properties.

Acknowledgements

This work was supported by the Chemical Biology Centre (Imperial College London) and the UK Engineering and Physical Sciences Research Council (EPSRC) Platform Grant EP/G00465X.

References

[1] Israelachvili, J.N. *Intermolecular and Surface Forces*, 2nd ed.; Academic Press: London, 1992.
[2] Evans, D.F.; Wennerström, H. *The Colloidal Domain: Where Physics, Chemistry, Biology, and Technology Meet*, 2nd ed.; Wiley-VCH: New York, 1999.
[3] Shearman, G.C.; Ces, O.; Templer, R.H.; Seddon, J.M. *J. Phys.: Condens. Matter* **2006**, *18*, S1105–S1124.
[4] Helfrich, W. *Z. Naturforsch., C: J. Biosci.* **1973**, *28*, 693–703.
[5] Helfrich, W. In *Physics of Defects*: Balian, R., Kleman, M., Poirer, J.P., Eds.; North Holland: Amsterdam, 1981; pp 713–756.
[6] Zimmerberg, J.; Kozlov, M.M. *Nat. Rev. Mol. Cell Biol.* **2006**, *7*, 9–19.
[7] Seddon, J.M.; Templer, R.H. *Philos. Trans. R. Soc. London, A* **1993**, *344*, 377–401.
[8] Saupe, A. *J. Colloid Interface Sci.* **1977**, *58*, 549–558.
[9] Huang, J.R.; Zou, L.N.; Witten, T.A. *Eur. Phys. J. E* **2005**, *18*, 279–285.
[10] Huang, J.R. *Eur. Phys. J. E* **2006**, *19*, 399–412.
[11] Lee, W.B.; Mezzenga, R.; Fredrickson, G.H. *Phys. Rev. Lett.* **2007**, *99*, 187801.
[12] Lee, W.B.; Mezzenga, R.; Fredrickson, G.H. *J. Chem. Phys.* **2008**, *128*, 074504.
[13] Seddon, J.M.; Zeb, N.; Templer, R.H.; McElhaney, R.N.; Mannock, D.A. *Langmuir* **1996**, *12*, 5250–5253.
[14] Duesing, P.M.; Seddon, J.M.; Templer, R.H.; Mannock, D.A. *Langmuir* **1997**, *13*, 2655–2664.
[15] Minamikawa, H.; Hato, M. *Langmuir* **1998**, *14*, 4503–4509.
[16] Seddon, J.M.; Robins, J.; Gulik-Krzywicki, T.; Delacroix, H. *Phys. Chem. Chem. Phys.* **2000**, *2*, 4485–4493.
[17] Mezzenga, R.; Ruokolainen, J.; Hexemer, A. *Langmuir* **2003**, *19*, 8144–8147.
[18] Murakami, Y.; Kikuchi, J.; Takaki, T.; Uchimura, K. *Bull. Chem. Soc. Jpn.* **1987**, *60*, 1469–1479.
[19] Duesing, P.M.; Templer, R.H.; Seddon, J.M. *Langmuir* **1997**, *13*, 351–359.
[20] Shearman, G.C.; Khoo, B.J.; Motherwell, M.L.; Brakke, K.A.; Ces, O.; Conn, C.E.; Seddon, J.M.; Templer, R.H. *Langmuir* **2007**, *23*, 7276–7285.
[21] Guillot, S.; Moitzi, C.; Salentinig, S.; Sagalowicz, L.; Leser, M.E.; Glatter, O. *Colloids Surf., A* **2006**, *291*, 78–84.
[22] Yaghmur, A.; de Campo, L.; Salentinig, S.; Sagalowicz, L.; Leser, M.E.; Glatter, O. *Langmuir* **2006**, *22*, 517–521.
[23] Salonen, A.; Guillot, S.; Glatter, O. *Langmuir* **2007**, *23*, 9151–9154.
[24] Pouzot, M.; Mezzenga, R.; Leser, M.; Sagalowicz, L.; Guillot, S.; Glatter, O. *Langmuir* **2007**, *23*, 9618–9628.
[25] Fontell, K. *Colloid Polym. Sci.* **1990**, *268*, 264–285.
[26] Shearman, G.C.; Tyler, A.I.I.; Brooks, N.J.; Templer, R.H.; Ces, O.; Law, R.V.; Seddon, J.M. *J. Am. Chem. Soc.* **2009**, *131*, 1678–1679.
[27] Fontell, K.; Fox, K.K.; Hansson, E. *Mol. Cryst. Liq. Cryst.* **1985**, *1*, 9–17.
[28] Vargas, R.; Mariani, P.; Gulik, A.; Luzzati, V. *J. Mol. Biol.* **1992**, *225*, 137–145.
[29] Delacroix, H.; Gulik-Krzywicki, T.; Mariani, P.; Luzzati, V. *J. Mol. Biol.* **1993**, *229*, 526–539.
[30] Delacroix, H.; Gulik-Krzywicki, T.; Seddon, J.M. *J. Mol. Biol.* **1996**, *258*, 88–103.
[31] Mariani, P.; Luzzati, V.; Delacroix, H. *J. Mol. Biol.* **1988**, *204*, 165–188.
[32] Sakya, P.; Seddon, J.M.; Templer, R.H.; Mirkin, R.J.; Tiddy, G.J.T. *Langmuir* **1997**, *13*, 3706–3714.
[33] Charvolin, J.; Sadoc, J.F. *J. Physique* **1988**, *49*, 521–526.
[34] de Geyer, A.; Guillermo, A.; Rodriguez, V.; Molle, B. *J. Phys. Chem. B* **2000**, *104*, 6610–6617.
[35] Mitchell, D.J.; Tiddy, G.J.T.; Waring, L.; Bostock, T.; McDonald, M.P. *J. Chem. Soc., Faraday Trans.* **1983**, *79*, 975–1000.
[36] Clerc, M. *J. Physique II* **1996**, *6*, 961–968.
[37] Zeng, X.B.; Liu, Y.S.; Impéror-Clerc, M. *J. Phys. Chem. B* **2007**, *111*, 5174–5179.
[38] Rodríguez, C.; Shigeta, K.; Kunieda, H. *J. Colloid Interface Sci.* **2000**, *223*, 197–204.
[39] Uddin, M.H.; Kanei, N.; Kunieda, H. *Langmuir* **2000**, *16*, 6891–6897.
[40] Kanei, N.; Watanabe, K.-I.; Kunieda, H. *J. Oleo Sci.* **2003**, *52*, 607–619.

[41] Kratzat, K.; Guittard, F.; de Givenchy, E.T.; Cambon, A. *Langmuir* **1996**, *12*, 6346–6350.
[42] Hossain, M.K.; Rodriguez, C.; Kunieda, H. *J. Oleo Sci.* **2004**, *53*, 35–39.
[43] Alexandridis, P.; Zhou, D.L.; Khan, A. *Langmuir* **1996**, *12*, 2690–2700.
[44] Alexandridis, P.; Olsson, U.; Lindman, B. *Langmuir* **1998**, *14*, 2627–2638.
[45] Svensson, B.; Alexandridis, P.; Olsson, U. *J. Phys. Chem. B* **1998**, *102*, 7541–7548.
[46] Hamley, I.W.; Daniel, C.; Mingvanish, W.; Mai, S.M.; Booth, C.; Messe, L.; Ryan, A.J. *Langmuir* **2000**, *16*, 2508–2514.
[47] Soni, S.S.; Brotons, G.; Bellour, M.; Narayanan, T.; Gibaud, A. *J. Phys. Chem. B* **2006**, *110*, 15157–15165.
[48] Deng, N.J.; Luo, Y.Z.; Tanodekaew, S.; Bingham, N.; Attwood, D.; Booth, C. *J. Polym. Sci., Part B: Polym. Phys.* **1995**, *33*, 1085–1096.
[49] Li, H.; Yu, G.E.; Price, C.; Booth, C.; Hecht, E.; Hoffmann, H. *Macromolecules* **1997**, *30*, 1347–1354.
[50] Bedells, A.D.; Arafeh, R.M.; Yang, Z.; Attwood, D.; Padget, J.C.; Price, C.; Booth, C. *J. Chem. Soc., Faraday Trans.* **1993**, *89*, 1243–1247.
[51] Auvray, X.; Petipas, C.; Anthore, R.; Ricolattes, I.; Lattes, A. *Langmuir* **1995**, *11*, 433–439.
[52] Auvray, X.; Petipas, C.; Dupuy, C.; Louvet, S.; Anthore, R.; Rico-Lattes, I.; Lattes, A. *Eur. Phys. J. E* **2001**, *4*, 489–504.
[53] Söderman, O.; Walderhaug, H.; Henriksson, U.; Stilbs, P. *J. Phys. Chem.* **1985**, *89*, 3693–3701.
[54] Balmbra, R.R.; Clunie, J.S.; Goodman, J.F. *Nature (London, UK)* **1969**, *222*, 1159–1160.
[55] Blackmore, E.S.; Tiddy, G.J.T. *J. Chem. Soc., Faraday Trans.* **1988**, *84*, 1115–1127.
[56] Rodríguez, C.; Kunieda, H. *Langmuir* **2000**, *16*, 8263–8269.
[57] de Geyer, A. *Prog. Colloid Polym. Sci.* **1993**, *93*, 76–80.
[58] Hagslätt, H.; Söderman, O.; Jönsson, B.; Johansson, L.B.A. *J. Phys. Chem.* **1991**, *95*, 1703–1710.
[59] Hagslätt, H.; Söderman, O.; Jönsson, B. *Langmuir* **1994**, *10*, 2177–2187.
[60] Kaneko, D.; Olsson, U.; Sakamoto, K. *Langmuir* **2002**, *18*, 4699–4703.
[61] Hagslätt, H.; Fontell, K. *J. Colloid Interface Sci.* **1994**, *165*, 431–444.
[62] Tardieu, A.; Luzzati, V. *Biochim. Biophys. Acta* **1970**, *219*, 11–17.
[63] Arvidson, G.; Brentel, I.; Khan, A.; Lindblom, G.; Fontell, K. *Eur. J. Biochem.* **1985**, *152*, 753–759.
[64] Eriksson, P.O.; Lindblom, G.; Arvidson, G. *J. Phys. Chem.* **1987**, *91*, 846–853.
[65] Eriksson, P.O.; Lindblom, G.; Arvidson, G. *J. Phys. Chem.* **1985**, *89*, 1050–1053.
[66] Lindblom, G.; Johansson, L.B.A.; Wikander, G.; Eriksson, P.O. Arvidson, G. *Biophys. J.* **1992**, *63*, 723–729.
[67] Birgbauer, E.; Chun, J. *Cell. Mol. Life Sci.* **2006**, *63*, 2695–2701.
[68] Nakano, T.; Inoue, I.; Shinozaki, R.; Matsui, M.; Akatsuka, T.; Takahashi, S.; Tanaka, K.; Akita, M.; Seo, M.; Hokari, S.; Katayama, S.; Komoda, T. *Biochim. Biophys. Acta* **2009**, *1788*, 2222–2228.
[69] King, M.D.; Marsh, D. *Biochemistry* **1989**, *28*, 5643–5647.
[70] Gulik, A.; Delacroix, H.; Kirschner, G.; Luzzati, V. *J. Physique II* **1995**, *5*, 445–464.
[71] Lindblom, G.; Rilfors, L. *Biochim. Biophys. Acta* **1989**, *988*, 221–256.
[72] Tardieu, A. Ph.D. Thesis, Universite de Paris-Sud, Orsay, France, 1972.
[73] Mariani, P.; Rivas, E.; Luzzati, V.; Delacroix, H. *Biochemistry* **1990**, *29*, 6799–6810.
[74] Seddon, J.M. *Biochemistry* **1990**, *29*, 7997–8002.
[75] Orädd, G.; Lindblom, G.; Fontell, K.; Ljusbergwahren, H. *Biophys. J.* **1995**, *68*, 1856–1863.
[76] Luzzati, V.; Vargas, R.; Gulik, A.; Mariani, P.; Seddon, J.M.; Rivas, E. *Biochemistry* **1992**, *31*, 279–285.
[77] Takahashi, H.; Hatta, I.; Quinn, P.J. *Biophys. J.* **1996**, *70*, 1407–1411.
[78] Huang, Z.; Seddon, J.M.; Templer, R.H. *Chem. Phys. Lipids* **1996**, *82*, 53–61.
[79] Seddon, J.M.; Bartle, E.A.; Mingins, J. *J. Phys.: Condens. Matter* **1990**, *2*, SA285–SA290.
[80] Tarahovsky, Y.S.; Koynova, R.; MacDonald, R.C. *Biophys. J.* **2004**, *87*, 1054–1064.
[81] Nieva, J.L.; Alonso, A.; Basanez, G.; Goni, F.M.; Gulik, A.; Vargas, R.; Luzzati, V. *FEBS Lett.* **1995**, *368*, 143–147.
[82] Minamikawa, H.; Hato, M. *Langmuir* **1997**, *13*, 2564–2571.
[83] Alexandridis, P.; Olsson, U.; Lindman, B. *Langmuir* **1996**, *12*, 1419–1422.
[84] Kraineva, J.; Nicolini, C.; Thiyagarajan, P.; Kondrashkina, E.; Winter, R. *Biochim. Biophys. Acta* **2006**, *1764*, 424–433.
[85] Mariani, P.; Amaral, L.Q.; Saturni, L.; Delacroix, H. *J. Physique II* **1994**, *4*, 1393–1416.
[86] Luzzati, V. *J. Physique II* **1995**, *5*, 1649–1669.
[87] Bang, J.; Lodge, T.P.; Wang, X.H.; Brinker, K.L.; Burghardt, W.R. *Phys. Rev. Lett.* **2002**, *89*.
[88] Bang, J.; Lodge, T.P. *J. Phys. Chem. B* **2003**, *107*, 12071–12081.
[89] Park, M.J.; Bang, J.; Harada, T.; Char, K.; Lodge, T.P. *Macromolecules* **2004**, *37*, 9064–9075.
[90] Rädler, J.O.; Radiman, S.; Devallera, A.; Toprakcioglu, C. *Phys. B (Amsterdam, Neth.)* **1989**, *156*, 398–401.
[91] Tansho, M.; Imae, T.; Tanaka, S.; Ohki, H.; Ikeda, R.; Suzuki, S. *Colloids Surf., B* **1996**, *7*, 281–286.
[92] Bull, T.; Lindman, B. *Mol. Cryst. Liq. Cryst.* **1974**, *28*, 155–160.
[93] Rilfors, L.; Eriksson, P.O.; Arvidson, G.; Lindblom, G. *Biochemistry* **1986**, *25*, 7702–7711.
[94] Lindblom, G.; Orädd, G. *Prog. Nucl. Magn. Reson. Spectrosc.* **1994**, *26*, 483–515.
[95] Leaver, M.; Rajagopalan, V.; Ulf, O.; Mortensen, K. *Phys. Chem. Chem. Phys.* **2000**, *2*, 2951–2958.
[96] Johansson, L.B.A.; Söderman, O. *J. Phys. Chem.* **1987**, *91*, 5275–5278.
[97] Hendrikx, Y.; Sotta, P.; Seddon, J.M.; Dutheillet, Y.; Bartle, E.A. *Liq. Cryst.* **1994**, *16*, 893–903.
[98] Kunieda, H.; Aramaki, K.; Izawa, T.; Kabir, M.H.; Sakamoto, K.; Watanabe, K. *J. Oleo Sci.* **2003**, *52*, 429–432.
[99] Francois, J. *J. Phys. Colloques* **1969**, *30*, 84–89.
[100] Francois, J. *Colloid Polym. Sci.* **1971**, *246*, 606–613.
[101] Photinos, P.; Melnik, G.; Saupe, A. *J. Chem. Phys.* **1986**, *84*, 6928–6932.

[102] Photinos, P.; Saupe, A. *Phys. Rev. A: At., Mol., Opt. Phys.* **1991**, *43*, 2890–2896.
[103] Photinos, P.; Saupe, A. *J. Chem. Phys.* **1981**, *75*, 1313–1315.
[104] Photinos, P.; Xu, S.Y.; Saupe, A. *Phys. Rev. A: At., Mol., Opt. Phys.* **1990**, *42*, 865–871.
[105] Photinos, P.J.; Saupe, A. *J. Chem. Phys.* **1984**, *81*, 563–566.
[106] Photinos, P.J.; Saupe, A. *J. Chem. Phys.* **1986**, *85*, 7467–7471.
[107] Photinos, P.J.; Saupe, A. *J. Chem. Phys.* **1986**, *84*, 517–521.
[108] Photinos, P.J.; Saupe, A. *Mol. Cryst. Liq. Cryst.* **1983**, *98*, 91–97.
[109] Photinos, P.J.; Yu, L.J.; Saupe, A. *Mol. Cryst. Liq. Cryst.* **1981**, *67*, 277–282.
[110] Lindblom, G.; Rilfors, L. *Biochim. Biophys. Acta* **1989**, *988*, 221–256.
[111] Cribier, S.; Bourdieu, L.; Vargas, R.; Gulik, A.; Luzzati, V. *J. Physique* **1990**, *51*, C7105–C7108.
[112] Cribier, S.; Gulik, A.; Fellmann, P.; Vargas, R.; Devaux, P.F.; Luzzati, V. *J. Mol. Biol.* **1993**, *229*, 517–525.
[113] Huo, Q.S.; Leon, R.; Petroff, P.M.; Stucky, G.D. *Science* **1995**, *268*, 1324–1327.
[114] Tolbert, S.H.; Schaffer, T.E.; Feng, J.L.; Hansma, P.K.; Stucky, G.D. *Chem. Mater.* **1997**, *9*, 1962–1967.
[115] Che, S.; Garcia-Bennett, A.E.; Yokoi, T.; Sakamoto, K.; Kunieda, H.; Terasaki, O.; Tatsumi, T. *Nat. Mater.* **2003**, *2*, 801–805.
[116] El-Safty, S.A.; Ismail, A.A.; Matsunaga, H.; Nanjo, H.; Mizukami, F. *J. Phys. Chem. C* **2008**, *112*, 4825–4835.